J. Chem. Chem. Eng. 7 (2013) 797-802

Heterogeneous Advanced Photo-Fenton Oxidation of Phenolic Aqueous Solutions over Iron-Containing SBA-15 Catalyst

Zohra Bailiche[1, 2], Leila Chérif-Aouali[1*], Sophie Fourmentin[2], Stéphane Siffert[2], Abdelkader Bengueddach[3] and Sébastien Royer[4]

1. Laboratory of Catalysis and Synthesis in Organic Chemistry, Tlemcen University, Tlemcen 13000, Algeria

2. UCEIV, Lille University, Lille F-59000, France

3. Laboratory of Materials Chemistry, Oran University, Oran 31000, Algeria

4. Institute of Chemistry, Poitiers University, Poitiers 86000, France

Received: December 13, 2012 / Accepted: January 07, 2013 / Published: September 25, 2013.

Abstract: Iron-containing SBA-15 catalysts have been prepared following different synthesis routes, direct synthesis by adjusting pH at 3 and 6 and with post synthesis procedure. Activity and stability of these materials were assessed on the photo-Fenton degradation of phenolic aqueous solutions by H_2O_2 using near ultraviolet irradiation (254 nm) at room temperature and initial neutral pH. Their catalytic performance was mentioned in terms of phenol and TOC (total organic carbon) conversions. Several complementary techniques, including X-ray, nitrogen sorption isotherms, UV (Ultraviolet) visible, were used to evaluate the final structural and textural properties of calcined Fe-SBA15 materials. These materials show a high activity and stability of iron species.

Key words: Fenton, photo-Fenton, mesoporous, Fe-SBA-15.

1. Introduction

Aromatic compounds are common pollutants in the effluents of several industries. The degradation of these pollutants in wastewater streams has emerged as an important concern during last decade. AOPs (advanced oxidation processes) such as ozonation, photocatalysis, Fenton and a combination of photo-Fenton, UV/O_3, UV/H_2O_2 have received considerable attention as wastewater treatment processes due to their ability to degrade, and in many cases, mineralize various organic compounds that are otherwise resistant to conventional biological and chemical treatments.

The oxidation system based on the Fenton's reagent (hydrogen peroxide in the presence of ferric ions) has been used as a powerful source of oxidative radicals [1].

$$Fe^{3+} + H_2O_2 \longleftrightarrow Fe(OOH)^{2+} + H^+ \quad (1)$$

$$Fe(OOH)^{2+} \longrightarrow Fe^{2+} + HO\cdot_2 \quad (2)$$

$$Fe^{2+} + H_2O_2 \longrightarrow Fe^{3+} + HO^- + HO\cdot \quad (3)$$

$$Fe^{3+} + HO\cdot_2 \longrightarrow Fe^{2+} + H^+ + O_2 \quad (4)$$

Fenton processes has been shown to be enhanced by light due to the decomposition of the photoactive $Fe(OH)^{2+}$ species, promoting an additional generation of OH· radicals in solution [2].

$$Fe(OH)^{2+} + h\nu \longrightarrow Fe^{2+} + HO\cdot \quad (5)$$

However, in order to overcome some drawbacks of this process (acidic pH requirement (pH = 2-4)), loss of Fe ions in water, etc., heterogeneous Fenton type systems have been synthesized to catalyse various organic compounds in mild reaction conditions.

The unique characteristics of mesoporous molecular sieves, such as high surface area, large pore volume

*Corresponding author: Leila Chérif-Aouali, Professor, research fields: heterogeneous catalysis, adsorption and nanostructured materials. E-mail: cherif_leila@yahoo.fr.

and well defined pore size, make the material potential in catalysis, adsorption, etc..

However, few investigations have been reported in using mesoporous materials for heterogeneous Fenton oxidation [3-6]. The purpose of this study is the assessment of Fe-containing SBA-15 mesostructured materials prepared by direct synthesis (by adjusting the pH at 6 and 3) and post synthesis procedures for the heterogeneous photo-Fenton degradation of phenolic aqueous solutions. Activity and stability of these materials have been evaluated according to the Si/Fe ratio 20 and 60.

2. Experimental Section

2.1 Mesoporous Materials Preparation

A detailed synthesis procedure for mesoporous silica SBA-15 has been reported elsewhere [7]. Iron substituted mesoporous SBA-15 molecular sieve has been prepared by direct synthesis at pH = 3 and 6 and post synthesis procedures using iron nitrate as source of iron.

2.1.1 Direct Synthesis

Fe-SBA-15 materials synthesized at pH = 3 were prepared as follows: 4.0 g triblock copolymer poly (propylene oxide)-poly (ethylene oxide) ($EO_{20}PO_{70}EO_{20}$ Pluronic 123 from Aldrich) was dissolved in 30.0 g of water and stirred for 4 h at 40 °C. 9.0 g of orthosilicate (TEOS) and the appropriate amount of iron nitrate were added directly to the homogeneous solution (Si/Fe = 20 and 60). Then appropriate quantity of 0.3 M HCl was added to adjust the pH value of mixture at 3.

The gel was stirred for 24 h and then maintained at 373 K in a Teflon-lined autoclave for another 48 h. The resultant precipitate was collected, washed thoroughly with distilled water; template removal was achieved by calcination in air at 500 °C for 4 h (heating rate: 1 °C/min).

Fe-SBA-15 materials synthesized at pH = 6 were prepared as follows: 4.0 g of triblock copolymer poly (propylene oxide)-poly (ethylene oxide) ($EO_{20}PO_{70}EO_{20}$ Pluronic 123 from Aldrich) was dissolved in 40 mL 2 M HCl and stirred for 30 min at 40 °C. 9.0 g of orthosilicate (TEOS) was added to the homogeneous solution. Then, appropriate quantity of 2 M NH_4OH were added to adjust the pH value of mixture to 6, then the appropriate amount of iron nitrate were added directly to the homogeneous solution in order to obtain a well defined Si/Fe = 20 and 60. The gel was stirred for 2 h and then maintained at 373 K in a Teflon-lined autoclave for three days.

The resultant precipitate was collected, washed thoroughly with distilled water; template removal was achieved by calcination in air at 500 °C for 4 h (heating rate: 1 °C/min). The samples were called FeSBA-15(n) where n represented the Si to Fe ratio.

2.1.2 Post-Synthesis

The calcined SBA-15 (0.5 g) was dispersed in 50 mL of deionised water containing various amounts of iron nitrate, in order to obtain a well defined Si/Fe ratio equal to 20 and 60.

The resulting mixture was stirred at room temperature for 12 h and the powder was filtered, washed with deionised water and dried at room temperature in air. The samples were called Fe/SBA-15 (*n*) where *n* is Si/Fe ratio.

2.2 Characterization

Various techniques including X-ray, N_2 adsorption and diffuse reflectance UV-vis (DRUV-vis) were employed for the materials characterization.

Heterogeneous photo-Fenton reaction were carried out in a cylindrical Pyrex reactors with one central and three peripheral female conical connections for the inflow and outflow of the solution model using phenol as reactant and hydrogen peroxide as oxidant.

The catalyst (100 mg) was put into 100 mL of an aqueous phenol solution (5×10^{-4} mol·L^{-1}) and the required amount of H_2O_2 was used for a complete phenol oxidation.

$$C_6H_5OH + 14H_2O_2 \longrightarrow 6CO_2 + 17H_2O \quad (6)$$

The reaction was carried out in ambient conditions

(atmospheric pressure, 25 °C and at neutral pH).

A dark Fenton were performed in atmospheric pressure, 25 °C and the pH of the reaction was maintained at 3.

Phenol conversions were determined by high performance liquid chromatograph (HPLC, waters 600) equipped with a C-18 column at a rate of 1 mL/min with UV detection with a mobile phase of 20% acetonitrile and 80% H_2O.

Iron leaching was systematically evaluated by ICP (induced coupled plasma) analyses model (820 MS Varian) after catalytic tests.

TOC (total organic carbon) content of the solutions after reaction was analysed using a Shimadzu TOC-VCSH analyzer.

3. Results and Discussion

Small angle X-ray diffraction patterns of the iron-containing SBA-15 materials are shown in Fig. 1. These materials exhibit a low angle reflections indexed as 100, 110 and 200 which can be associated with the hexagonal symmetry characteristic of mesoporous SBA-15. The authors can note that co-condensed materials (Fe-SBA-15) are not as highly ordered as impregnated materials Fe/SBA-15. The XRD patterns of Fe-SBA-15 show that the peaks 110 and 200 are not well resolved whatever the synthesis pH value and Si/Fe ratio are. This could be explained by the lattice distortion after insertion of Fe. Since the radius of the ionic Fe^{3+} (r_{Fe}^{3+} = 0.63 Å) is larger than that of Si^{4+} (r_{Si}^{4+} = 0.40 Å), the increase in the unit cell parameter value of the Fe-SBA-15(60) material (Table 1) may indicate that Fe^{3+} ions are incorporated into the framework of the SBA-15 material; generally, it is expected that the unit cell parameter will be enlarged after the incorporation of metal cations with ionic radius larger than that of Si^{4+}. However, the Fe rich containing SBA15 (FeSBA-15(20)) presents a decrease in its unit cell parameter; this result could be attributed to a partiel collapse of hexagonal porosity caused by the modification induced by the iron introduction in the mesoporous silica structure [8, 9].

In all cases, the absence of diffraction peaks at $2\theta > 10°$ seems to exclude the presence of Fe_2O_3 crystallites or in too low quantity to be observed.

Typical irreversible type IV (four) adsorption isotherms as defined by IUPAC (International Union of Pure and Applied Chemistry) [10] were observed which is typical of mesoporous materials (Fig. 2). The N_2 isotherms remained unchanged in shape for impregnated materials Fe/SBA-15 and co-condensed materials (FeSBA-15) at pH = 6 compared to that of SBA-15. By contrast, the N_2 isotherms were less sharp for co-condensed materials (FeSBA-15) at pH = 3 indicating that the materials were less ordered and uniform compared to SBA-15.

The surface area values of purely siliceous SBA-15 and FeSBA-15 materials are listed in Table 2. The decrease in the BET surface area of SBA-15 when iron was introduced could be partly attributed to clogging support pores by iron species that makes them inaccessible for nitrogen adsorption.

Diffuse reflectance UV-vis spectroscopy was used to investigate the nature of the Fe (III) species.

The DR (diffuse reflectance) UV-vis spectra of synthesized and calcined FeSBA-15 samples are shown in Fig. 2.

The spectra of as synthesised FeSBA-15 (Si/Fe = 20 and 60) synthesized at pH = 6 show two absorption

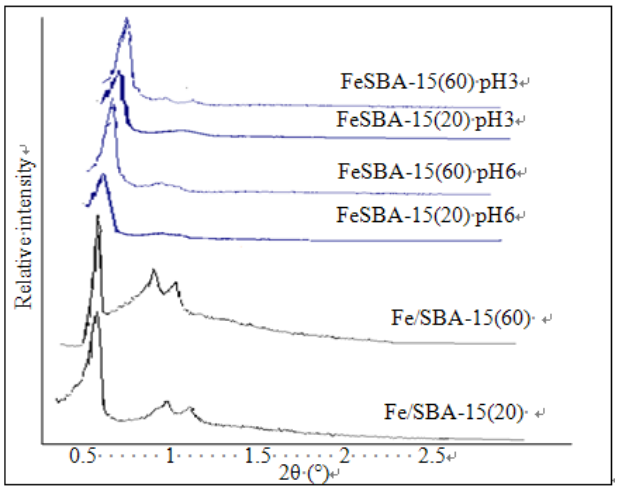

Fig. 1 XRD profiles of FeSBA-15.

Table 1 Physical properties of the calcined FeSBA-15.

Sample	SBA-15	Fe/SBA-15		FeSBA-15 synthesized at pH6		FeSBA-15 synthesized at pH3	
Si/Fe		20	60	20	60	20	60
*d*100 (Å)	96	103.8	101.4	91.9	101.5	92.3	103.7
a (Å)	110.8	119.9	117.1	106.1	117.2	106.6	119.7

Table 2 Specific surfaces of FeSBA-15.

Sample		Fe/SBA-15	FeSBA-15 synthesized at pH6		FeSBA-15 synthesized at pH3	
Si/Fe	20	60	20	60	20	60
S (m^2/g)	732	601	822	623	502	895

bands below 250 nm (210 nm, 240 nm), two bands between 300 and 400 nm. The bands below 250 nm are attributed to isolated Fe^{3+} in tetrahedral coordination and those between 300 nm and 400 nm are attributed to iron oxide nanoclusters (Fe_xO_y) [11]. Both samples are free of large Fe_2O_3 as evidenced by missing bands above 400 nm.

The DR UV-vis spectra of calcined FeSBA-15 samples synthesized at pH = 6 (Fig. 3) show the exaltation of the band attributed to Fe^{3+} in tetrahedral coordination (< 250nm), disappearance of bands attributed to nanoclusters of iron oxide (300-400 nm) and the appearance of a band at 250 nm (< 300 nm) attributed to Fe^{3+} in octahedral coordination. This result can be explained by the redispersion of the iron species and their partial insertion into the framework. After calcination of the FeSBA-15 materials, the insertion of iron into the framework after calcination is in contradiction with what is usually observed with mesoporous materials exchanged by metal.

The spectra of synthesized and calcined FeSBA-15 (Si/Fe = 20) synthesized at pH = 3 (Fig. 4) show two absorption bands; the first is attributed to Fe^{3+} in tetrahedral coordination (< 250 nm) and the second is attributed to nanoclusters of iron oxide (300-400 nm).

Activity and stability of catalytic systems in photoassisted oxidation of phenolic aqueous solutions: Table 3 summarizes the activity of all the catalysts prepared during this study in the photo-Fenton of phenol degradation at different reaction times. A nearly total phenol removal is displayed by all

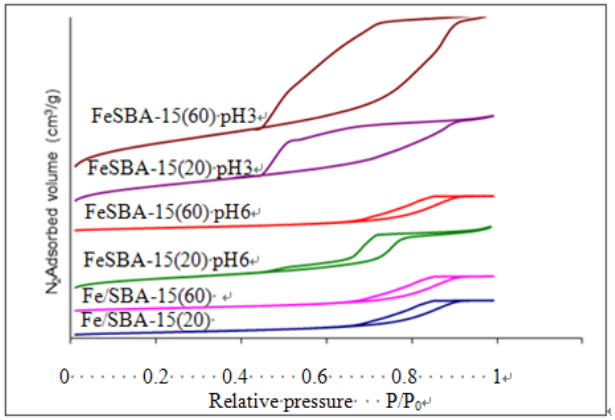

Fig. 2 Adsorption-desorption isotherms of nitrogen on FeSBA-15.

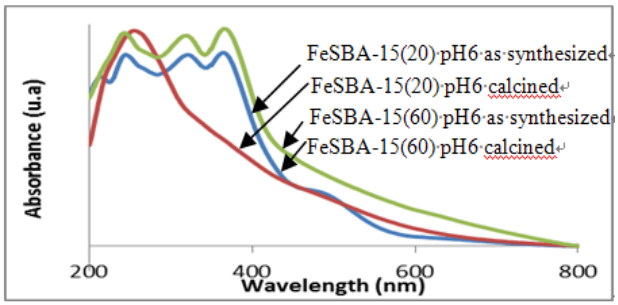

Fig. 3 The diffuse reflectance UV-visible spectra of FeSBA-15(n) pH6.

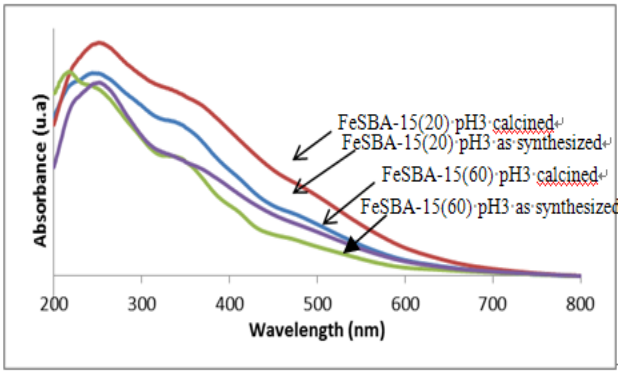

Fig. 4 The diffuse reflectance UV-visible spectra of FeSBA-15(n) pH3.

Table 3 Activity of catalysts FeSBA-15.

Sample	*t* (min)	Phenol conversion (%)	Iron Leaching (%)	TOC (%)[a]
Fe/SBA-15(20)	0	0	33.3	13.3
	5	93.9		
	10	98.7		
	15	100		
Fe/SBA-15(60)	0	0	-	16.3
	5	84.0		
	10	96.2		
	15	100		
FeSBA-15(20) synthesized at pH6	0	0	22.5	5.3
	5	90.5		
	10	100		
	15	100		
FeSBA-15(60) synthesized at pH6	0	0	15.9	7.3
	5	90.0		
	10	100		
	15	100		
FeSBA-15(20) synthesized at pH3	0	0	17.0	11.4
	5	90.7		
	10	100		
	15	100		
FeSBA-15(60) synthesized at pH3	0	0	15.0	9.6
	5	79.2		
	10	96.7		
	15	100		

[a]: TOC (total organic carbon) abatement level

samples after reaction times of 10 min. Table 3 shows the effect of Si/Fe ration and the synthesis procedure of FeSBA-15 on phenol degradation, suggesting in the case of FeSBA-15 synthesized at pH = 3 that the decrease in Si/Fe from 60 to 20 accelerate the oxidation of phenol since more radicals are produced from higher iron loaded catalysts. However, in the case of FeSBA-15 synthesized at pH = 6 and Fe/SBA-15 synthesized by post-synthesis procedure, the oxidation of phenol is not accelerated with the decrease in Si/Fe from 60 to 20; Therefore Si/Fe = 60 is the optimum value and 100% of phenol has been degraded after reaction time of 10 min with FeSBA-15 synthesized at pH = 6. It has been demonstrated that the photo-Fenton activity of a catalyst can be influenced by its surface area, crystal structure, particle size distribution or surface hydroxyl group density [12].

Comparing values of TOC degradation for catalysts a high activity of FeSBA-15 synthesized at pH = 6 is obtained. An important point in the design of heterogeneous catalytic systems for advanced oxidation processes is the resistance of metal species to be leached into the aqueous solution under the oxidant; in this sense, stability of all the materials was evaluated in the terms of the percentage of iron leached from the catalyst with the reaction time. The catalyst Fe/SBA-15(20), synthesized by post-synthesis procedure, shows a higher leaching degree in comparison to those obtained by direct synthesis, which are mainly composed of framework iron which is more resistant to be leaching out into the aqueous solution.

3.1 Study of Parallel Reactions on the Phenol Photo-Degradation

The influence of parallel reactions such as

dark-Fenton, degradation mediated by photolysis of H_2O_2 and adsorption phenomenon on the overall degradation of phenol has been studied. The results show that mineralization of phenol towards carbon dioxide and water by irradiated homogeneous Fenton catalytic systems and UV/H_2O_2 processes may occur along with heterogeneously Fenton photo-assisted reactions, but the remarkable contribution of iron containing SBA-15 catalyst is undoubtedly demonstrated.

3.2 Study of Stability of Catalysis

The performance of FeSBA-15(60) synthesized at pH = 6 in phenol degradation after catalyst recycling with filtration and water washing is similar to the first test; this suggests the stable performance of FeSBA-15(60) in heterogeneous Fenton oxidation.

4. Conclusions

A series of iron-based mesoporous materials were prepared following different routes. FeSBA-15 prepared by direct synthesis is not as highly ordered as impregnated materials Fe/SBA-15.

It is worth noting that after calcination of FeSBA-15 synthesized at pH = 6, the extra framework iron species are redispersed and partially inserted into the framework. Activity and stability of FeSBA-15 for treatment of phenolic aqueous solutions depend on the synthesis strategy and Si/Fe ratio.

FeSBA-15(60) synthesized at pH = 6 is a promising catalyst for photo-Fenton processes.

References

[1] Walling, C.; Goosen, A. Mechanisms of the Ferric Ion Catalyzed Decomposition of Hydrogen Peroxide and Effect of Organic Substrates. *J. Am. Chem. Soc.* **1973,** *95,* 2987-2991.

[2] Nadtochenco, V. Photolysis of $FeOH^{2+}$ and $FeCl^{2+}$ in Aqueous Solution, Photo Dissociation Kinetics and Quantum Yields. *Inorg. Chem.* **1998,** *37,* 5233-5238.

[3] Gokulakrishnan, N.; Pandurangan, A.; Sinha, P. K. Removal of Citric Acid from Aqueous Solution by Catalytic Wet Peroxidation Using Effective Mesoporous Fe-MCM-41 Molecular Sieves. *Journal of Chemical Technology and Biotechnology* **2007,** *82,* 25-32.

[4] Martinez, F.; Calleja, G.; Melero, J. A.; Molina, R. Heterogeneous Photo-Fenton Degradation of Phenolic Aqueous Solutions over Iron-Containing SBA-15 Catalyst. Applied Catalysis B. Environmental **2005,** *60,* 181-190.

[5] Xiang, L.; Royer, S.; Zhang, H.; Tatibouët, J. M. Properties of Iron-Based Mesoporous Silica for the CWPO of Phenol: A Comparison between Impregnation and Co-Condensation Routes. *Journal of Hazardous Materials* **2009,** *172,* 1175-1184.

[6] Shukla, P.; Wang, S.; Sun, H.; Ang, H. M.; Tadé, M. Adsorption and Heterogeneous Advanced Oxidation of Phenolic Contaminants Using Fe Loaded Mesoporous SBA-15 and H_2O_2. *Chemical Engineering Journal* **2010,** *164,* 255-260.

[7] Zhao, D.; Feng, J.; Huo, Q.; Melosh, N.; Frederickson, G. H.; Chmelka, B. F.; et al. Triblock Copolymer Syntheses of Mesoporous Silica with Periodic 50 to 300 Angstrom Pores. *Science* **1998,** *279,* 548-552.

[8] Berrichi, Z. E.; Cherif, L.; Orsen, O.; Fraissard, J.; Tessonnier, J. P.; Vanhaecke, E.; et al. Ga Doped SBA-15 as an Active and Stable Catalyst for Friedel-Crafts Liquid-Phase Acylation. *Appl. Catal. A* **2006,** *298,* 194-202.

[9] Cheng, C. F.; Albo, M. D.; Klouski, J. The Unit Cell of the Gallosilicate Mesoporous Molecular Sieve [Si, Ga]-MCM-41 is Significantly Smaller than in the Purely Siliceous [Si]-MCM-41. *Chem. Pyhys. Lett.* **1996,** *250,* 328-334.

[10] Colloid and Surface Chemistry. In *IUPAC Manual of Symbols and Terminologie;* 1972; Vol. 31, p 578.

[11] Bordiga, S.; Buzzoni, R.; Geobaldo, F.; Lamberti, C.; Giamello, E.; Zecchina, A.; et al. Structure and Reactivity of Framework and Extraframework Iron in Fe-Silicalite as Investigated by Spectroscopic and Physicochemical Methods. *J. Catal.* **1996,** *158,* 486-501.

[12] Bahnemann, D. W. *Photochemical Conversion and Storage of Solar Energy;* Kluwer Academic Publishers: Dordrecht, 1991; pp 251-276.